INTERNATIONAL JOURNAL OF APPLIED RESEARCH ON TEXTILE
URL: http://atctex.org/ijartex
Volume 2, Issue 1, pp 18-29, April 2014

ADHESION CHARACTERIZATION OF ALFA FIBRES IN UNSATURATED POLYESTER MATRIX

TRIKI A.[1]*, OMRI MED A.[1], GUICHA M.[2], BEN HASSEN M.[2], AROUS M.[1] AND KALLEL A.[1]

[1]CERAMICS MATERIALS, COMPOSITES AND POLYMERS LABORATORY, FSS 3018, TUNISIA
[2]TEXTILE ENGINEERING LABORATORY, UNIVERSITY OF MONASTIR, TUNISIA

Received 13 September 2013, Accepted 09 March 2014

ABSTRACT

Polymer composite of an unsaturated polyester matrix with non-woven Alfa fibres hybridized with wool fibres and thermo-binder fibres (PE/PET) was characterized by different techniques in order to analyze the interfacial region fibres/matrix. Dielectric measurements were performed in the frequency range 0.1 Hz - 1 MHz and temperature interval from 40 to 150°C. This study allowed the analysis of the interfacial or Maxwell-Wagner-Sillars (MWS) polarization effect using the Havrilliak Negami equation adopting the electric modulus formalism. The lowness of this relaxation intensity revealed an adhesion of the fibres in the matrix. These results were confirmed by FT-IR technique that demonstrated a chemical mechanism of adhesion based on covalent bonds and on hydrogen bridges. In addition, the Scanning Electron Microscope (SEM) observation showed that a close contact could happen between the fibres and the matrix.

KEYWORDS

SEM; Relaxation; FT-IR; Alfa; Non-woven fibres

1. INTRODUCTION

The use of natural fibres has gained attention due to the reduction of waste disposal problems especially in agricultural fields and environmental pollution and can find various applications in engineering, electronic and automotive fields [Ermolaeva, 2002]. Green, environmentally friendly, sustainable, renewable, biodegradable composites from natural fibers are among the most keenly required materials nowadays. Most cellulosic fibres are harvested yearly and the supply should be inexhaustible compared to the limited supply of oil reserve from which many synthetic fibres are derived. Natural fibres reinforced polymers also have exhibited numerous advantages such as high mechanical properties, low weight, low cost, low density, high specific properties, possess better electrical resistance, good thermal and acoustic insulating properties and higher resistance to fracture. Additionally, the natural fibres reinforced composites can decrease wearing of machines due to its low abrasiveness and absence of health hazardness during processing, application and upon disposal. Natural fibres such as hemp, sisal, flax, kenaf and jute are highly hydrophilic due to the presence of hydroxyl groups (OH) which present a low compatibility with the hydrophobic matrix. To overcome this poor compatibility many experimental treatments have been developed such as the suitable modification of fibres surface [Laly, Sabu, 2003, Bisanda, Anshell, 1991], or by using coupling agent [Ghallabi, 2010] or by modifying matrix to make it more compatible with cellulose fibres [Aziz , 2005]. It was also demonstrated that the amount of moisture sorption could be significantly reduced by replacing natural fibres with a small amount of synthetic fibres such as glass or carbon [Mishra, 2003].

* : Corresponding author. Email : trikilamacop@yahoo.fr

In the present work, we were interested about the adhesion of Alfa fibres in the unsaturated polyester matrix. In this study, we tried to take into account the hybrid character of the composite with two natural fibres (Alfa and wool) and polymeric fibres (PET/PE) which act as thermo-binder fibres. Many experimental techniques were performed in this study such as dielectric analyser (DEA), Fourier transform infrared spectroscopy (FT-IR) and Scanning Electron Microscopy (SEM).

2. EXPERIMENTAL

2.1. Materials

Alfa fibres extracted from the plant were attacked chemically by a sodium hydroxide solution and were bleached in a NaClO solution. Such alkali treatment could enhance the number of available OH groups due to the removal of pectin and waxy materials from the fibres surfaces. Furthermore, bleaching Alfa fibres might also remove some materials of high water adsorption. Hence, it could be believed that the increased exposure of the OH groups of fibres provided improved potential for hydrogen and covalent bonding with the carbonyl (C=O) and carboxyl (COOH) groups of the matrix, respectively [Moyeenuddin, 2011].These fibres were then separated mechanically twice by means of a Shirley analyzer [Guicha, 2009]. As the elaboration of non-woven fibres with only Alfa fibres were not possible due to the non-cohesion between fibres, these fibres were mixed with wool fibres to assure the cohesion. Thermo-binder fibres composed of PET and PE as a cover were added in the reinforcement in order to be thermoformed. The obtained sheet of nonwoven fibres was made up of these three kinds of fibres (Alfa/wool and thermo-binder (PE/PET)) in the relative fraction of 85, 10 and 5 %, respectively, i. e. 17:2:1. The polymer used as a matrix in our composite is the unsaturated polyester (UP) resin "NORSODYNE H13372 TAE". The composite was prepared using the classical "contact method" [Guicha, 2009]. Indeed, the reinforcement was deposited on the mould and impregnated with the liquid resin mixed with suitable proportions of Methyl ethyl Ketone peroxide and Cobalt octanone as hardener and catalyst, respectively. The saturated material was then pressed by a roller to remove bubbles. After the hardness of the resin, the composite was withdrawn from the mould. The used reinforcement has a surface weight of 326 g/m^2. The obtained composite has a surface weight of 6363,64 g/m^2. The weight fraction of the composite was calculated according to the following equation:

$$\varphi_m = \frac{surface\ weight\ of\ the\ reinforcement}{surface\ weight\ of\ the\ composite} \quad (1)$$

The weight fraction of the composite is about 5.13 %. This reinforcement may alter the molecular dynamic of the polymer which gives rise to different dielectric relaxations depending on the temperature range. Figure 1-(a, b) illustrates photos of the reinforcement and the composite, respectively.

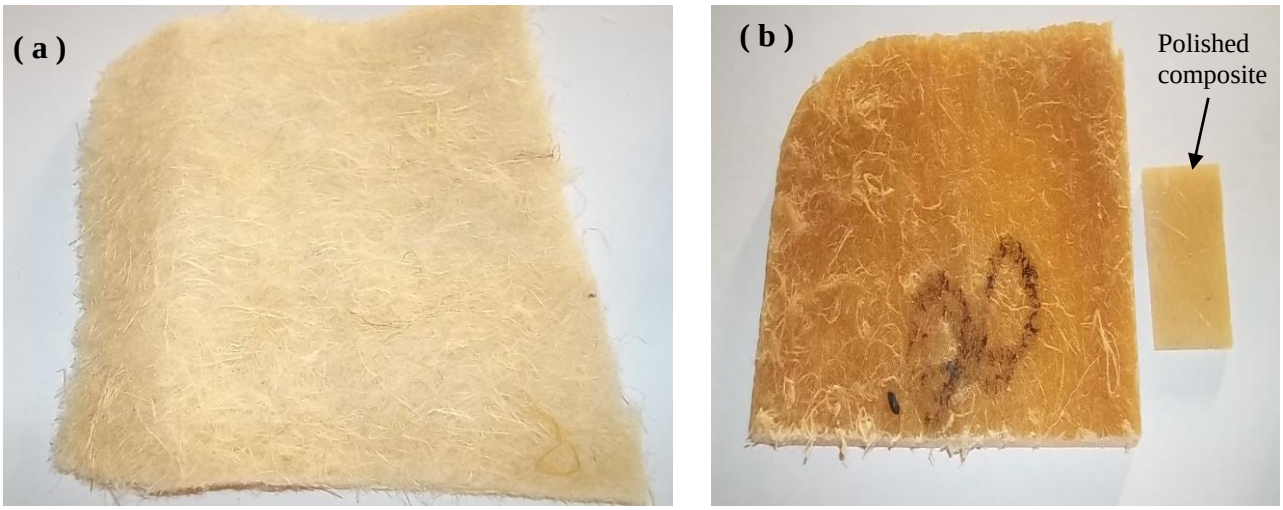

Figure 1: Photos of the reinforcement (a) and the composite (b)

2.2. Equipment

Dielectric method was interrelated to the Infrared spectroscopy in order to study the adhesion of the reinforcement in the unsaturated polyester matrix [Arous, 2007, Ghallabi, 2010, Triki, 2011].
Dielectric measurements were performed by means of a Novocontrol system integrating ALFA dielectric interface over a broad frequency window, 10^{-1} < f(Hz) < 10^{6}. As thermal properties of the unsaturated polyester matrix revealed a glass transition temperature of about 68°C [Triki, 2011] and taking into account either the hydrophilic character of natural fibres or their decomposition temperature, these measurements were taken over the temperature range from 40°C to 150°C so that low and high temperatures dielectric relaxations could be analyzed and decomposition of the reinforcement could be avoided.
According to this characterization, an electric field was applied across the faces of a parallel plate capacitor containing the composite which polarized it. Different polarization mechanisms could happen but in dielectric spectroscopy the major polarization mechanisms that could be studied are polarization due to charge migration and polarization due to orientation of permanent dipoles. The first one could give rise to the conductivity originating from ionic impurities and the interfacial polarization due to the built up of charges at the interface between components in the studied sample. These polarizations occurred at higher temperatures above the glass transition temperature. The second polarization was produced as a result of the alignment of dipoles in the direction of the applied electric field which involved cooperative motions of molecular segments. The most attractive features of the dielectric spectroscopy lies in its applicability to the studies aimed at the development of direct correlations between the response of a real system and an idealized model circuit composed of discrete electrical components. For frequency below 10^{8} Hz, it is convenient to use equivalent electrical circuits made up of resistors and capacitors. The resistance is taken to represent the dissipative component of the dielectric response, while a capacitance describes the storage components of the dielectric. The measuring impedance analyzer will measure a sample with parallel plate as a resistor R_P in parallel with a capacitor C_P. The equivalent electrical circuit is illustrated in figure 2. For ac measurements the corresponding electrical admittance was given by the following equation:

$$Y(\omega) = G_P(\omega) + i\,\omega C_P(\omega). \tag{2}$$

Where $G_P(\omega)$ (= $\frac{1}{R_P}$) is the parallel conductance and ω is the angular frequency (= 2 π f). The measured value of the admittance depends on the geometry of the sample (sample area A and the thickness d for a parallel-plate cell). The empty dielectric cell has a geometrical capacitance given by $C_o = \frac{A\,\varepsilon_o}{d}$, where $\varepsilon_o$is the permittivity of free space. The expression of the electrical admittance is often reported in terms of the complex dielectric constant as follows:

$$\varepsilon^*(\omega) = \frac{Y(\omega)}{i\,\omega C_o} = \varepsilon' - i\,\varepsilon'' \tag{3}$$

Where i is $(-1)^{\frac{1}{2}}$, $\varepsilon'$and ε'' are the real and the imaginary parts of the complex permittivity (ε^*). These parameters are obtained according the following equations [Belaabed, 2011]:

$$\varepsilon' = \frac{C_P\,d}{\varepsilon_o\,A} \tag{4}$$

$$\varepsilon'' = \frac{G_P\,d}{\omega\,\varepsilon_o\,A} \tag{5}$$

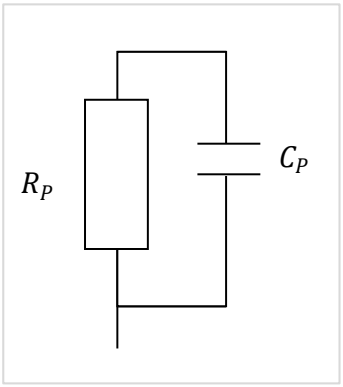

Figure 2: Circuit diagram for the modelling of material properties

FT-IR measurements were performed using a Perkin Elmer FT-IR spectrometer. A total of 10 scans were taken for each sample with a resolution of 2 cm^{-1}. Ground dried sample and KBr (5 mg sample per 100 mg KBr) were pressed into a disk for FT-IR measurement. According to this characterization, an infrared radiation passes through the sample and it is absorbed selectively at certain frequencies. Hence each change of the atomic dipole moment in the polymer gives rise to an IR peak which resonant frequency occurs at infrared range 400-4000 cm^{-1}.
To further support these analytical experimental studies, the morphology of the composite surfaces was observed at room temperature by SEM PHILIPS XL30. A gold coating of a few nanometers in thickness was formed on the surfaces of the samples to prevent charging.These observations were conducted on the cross section surface of the composite so that the cross section aspects of the fibres could be shown and hence the surrounding regions of the reinforcement fibre in the matrix could be observed.

3. RESULTS AND DISCUSSION

3.1. DEA

The real part of permittivity ε' and the dissipation factor $\tan\delta$ versus frequency for the composite are shown in figure 3-(a, b), for different temperatures varying from 40 to 150 °C in increments of 10°C. For low frequencies, the permittivity reached high values when temperatures increased. The high value at low temperatures of ε' is due to the presence of water and impurities present in the reinforcement fibres [Arous, 2007]. The increase of the temperature leads to the increase of ε' due to the enhanced conductivity of the composite and the interfacial polarization effect at higher temperatures.
The analysis of the dissipation effect confirms the presence of the two dielectric relaxations. Indeed, the one appeared at low temperatures was attributed to the water dipoles polarisation. Similar results were obtained in natural fibres reinforced polymeric matrix [Arous, 2007]. Meanwhile, the second one exhibited at low frequencies and high temperatures was associated to the interfacial polarization effect. We can notice an enhancement of the dissipation factor at low frequencies attributed to the dc conductivity. As the interfacial polarization effect and that of conductivity originate from charged carrier mobility the formalism of the 'electric modulus' or 'inverse complex permittivity' is introduced in order to minimize the dc conductivity effect. The electric modulus, M^*, is defined by the following Eq. 6 [Howard, 1992]:
$M^* =$

$$\frac{1}{\varepsilon^*}=\frac{1}{\varepsilon^{'}-j\varepsilon^{''}}=\frac{\varepsilon^{'}}{\varepsilon^{'2}+\varepsilon^{''2}}+j\frac{\varepsilon^{''}}{\varepsilon^{'2}+\varepsilon^{''2}}$$

$$=M^{'}+jM^{''} \qquad (6)$$

where M' and M" are the real and the imaginary parts of electric modulus respectively. In figure 4 is depicted the isothermal runs of M" as a function of the frequency when the composite is heated over the temperature range from 40°C up to 150°C. These presentations confirm the presence of the water dipoles polarization at low temperatures and that of the interfacial polarization effect at high temperatures. An additional dielectric relaxation observed above glass transition temperature was associated with the α relaxation of the matrix. Such dielectric relaxation cannot be observed on the dissipation factor presentations as it is hidden by the interfacial polarization effect. These attributions were supported by the evaluation of the activation energy of each dielectric relaxation done previously [Triki, 2013]. Accordingly, the analysis of the activation energy E_a^{α} of the α relaxation revealed an interaction between the reinforcement and the matrix [Triki, 2013].

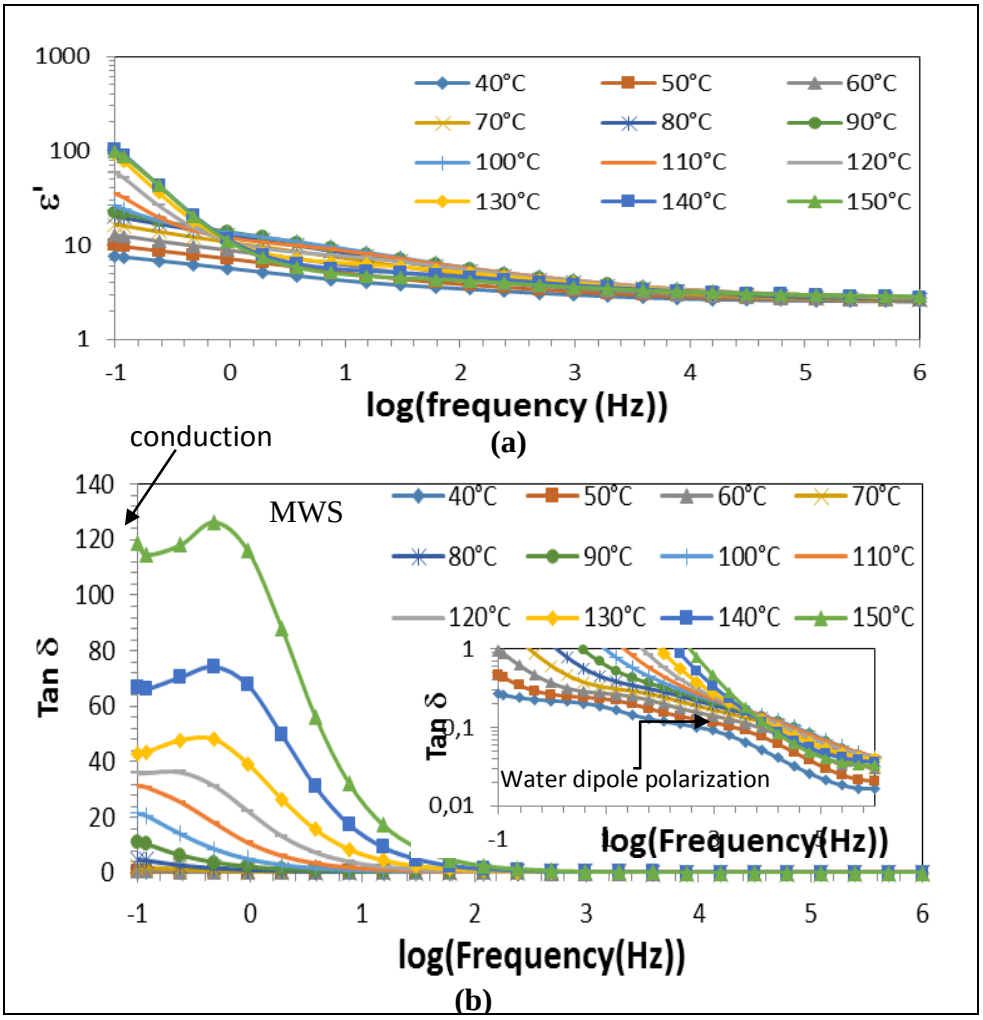

Figure 3: Isothermal runs of the dielectric permittivity ε' (a) and the dissipation factor (b) versus frequency of the composite

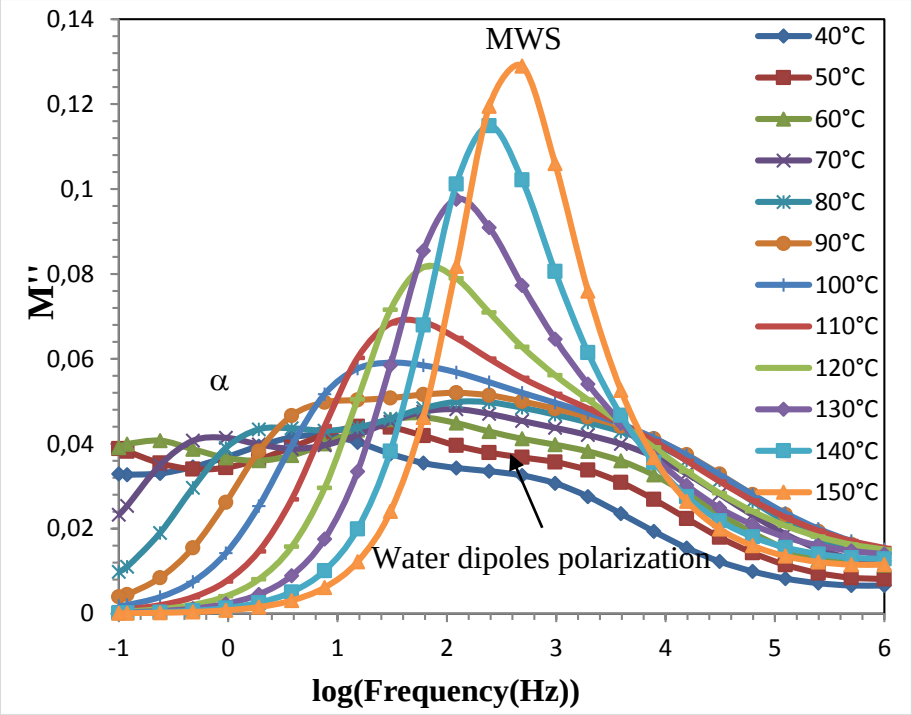

Figure 4: Isothermal runs of the imaginary part of the electric modulus M'' versus frequency of the composite

Furthermore, the use of the Argand representation (Cole–Cole diagram) provides interesting knowledge regarding the nature of relaxation. Cole–Cole plots of the composite at 150 °C are depicted in figure 5. Havriliak–Negami model fits correctly the data [Havriliak, Negami, 1966, Wagner, H. Richert, R. 1999].

$$M^*(\omega) = M_\infty + \frac{M_s - M_\infty}{\left(1 + (i\omega\tau)^{1-\alpha}\right)^\beta} \tag{7}$$

Where α and β are relaxation exponents, and M_s and M_∞ are the modulus at low and high frequencies, respectively. We notice that it was impossible to fit to the Havriliak–Negami model with all the experimental points. Similarly, it can be noticed that at low frequencies domain (lower values of M' and M''), the experimental points reach the origin of the graph, which is a typical behaviour of dc conduction effect. So, two semicircles are obtained in every examined temperature. The first one for 0 < M' < 0.23 is related to the conduction effect and the second one for 0.23 < M' < 0.33 is attributed to the MWS effect. The parameters evaluated by the fitting data are listed in Table 1. To determine the parameters characteristics of the Havriliak-Negami model (α, β, M_s, M_∞), the experimental M'_{exp} and M''_{exp} data were smoothed through a numerical simulation in the complex plane. The purpose of such a simulation was to find out the theoretical values (M'_{th} and M''_{th}). The values of α, β, M_S and M_∞ that best smoothed the Havriliak-Negami data were obtained by a successive approach method, in which the following expressions were minimized :

$$\chi^2_{M'} = \sum_i (M'_{th} - M'_{exp})^2 \tag{8}$$

$$\chi^2_{M''} = \sum_i (M''_{th} - M''_{exp})^2 \tag{9}$$

It has been proven that only one quadruplet value to tone with these conditions. The values of α and β obtained for conductive effect are in harmony with a pure Debye-type for the composite. Meanwhile, the

values of α and β obtained for MWS polarization effect go in the same line with the Havriliak–Negami response.

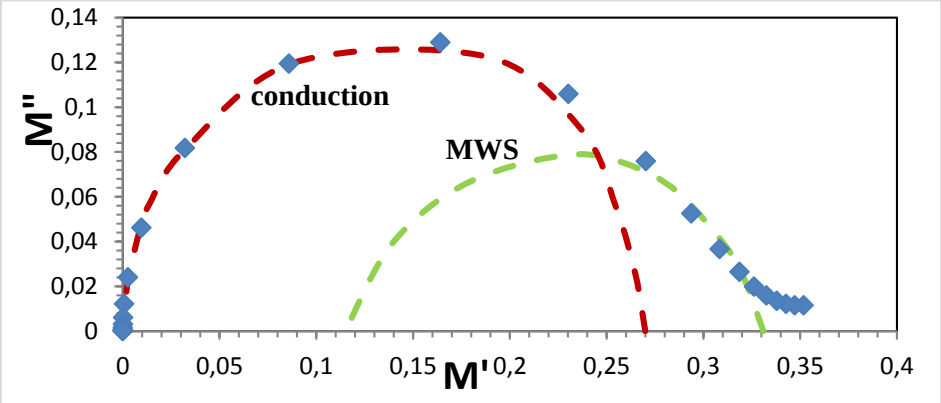

Figure 5: Argand's plots of the electric modulus, M* of the composite at 150°C

Table 1: Parameters evaluated by data fitting according to the Havriliak–Negami equation for the composites

Sample	T (°C)	relaxation	α	β	M_S	M_∞
Composite	120	Conduction	0.9957	0.889	0.0052	0.31
		MWS	0.92	0.892	0.199	0.315
	130	Conduction	0.995	0.83	0.005	0.32
		MWS	0.92	0.892	0.199	0.315
	140	Conduction	0.999	0.819	0.00399	0.3269
		MWS	0.92	0.892	0.199	0.315
	150	Conduction	0.945	0.879	0.003	0.33
		MWS	0.92	0.892	0.199	0.315

Table 2 presents the interfacial relaxation strength of MWS relaxation in permittivity values defined by ($\Delta\varepsilon = \varepsilon_s - \varepsilon_\infty$) [Puertolas, 1999] .From this Table, we notice that the relaxation strength of MWS relaxation increases with temperature. This can be due to the increase in free charges, which come to be blocked in greater numbers at the interfaces, thus increasing the aptitude of the dipoles to be polarized. In addition, these values are lower and this is attributed to the interaction between the fibres and the matrix as mentioned above.

Table 2: Interfacial relaxation strength

Sample	T (°C)	Δε
Studied composite	120	2.69
	130	4.11
	140	6.00
	150	5.67

3.2. FT-IR

The reinforcement of the composite by three types of fibres leads to a hybrid composite with a great diversity of material properties. Hence, the presence of wool and thermo-binder may improve Alfa fibres hydrophobic nature, surface roughness, wettability and interfacial bonding between matrix and fibres despite of the hygroscopic character of wool fibres which have hydrophobic surfaces. FT-IR spectra of the reinforcement and its constituents are presented in figure 6. The main absorption peaks obtained for the Alfa fibres are as follows: (i) the peak around 3378 cm^{-1} which can be attributed to the stretching vibrations of hydroxyl (OH) groups; (ii) strong peak at 2913 cm^{-1} assigned to methylene C-H asymmetric stretching

vibration of cellulose; (iii) the peak at 1646 cm^{-1} attributed to the stretching vibration of water molecules due to the hydrophilic character of the lingo-cellulosic fibers; (iv) the bands at 1455 and 1430 cm^{-1} due to the C=C bond elongation of the lignin aromatic ring [Sun, 2005]; (v) the band at 1376 cm^{-1} associated with vibrational perturbations of glycosidic bonding in the cellulose backbone [Colom, 2003]; (vi) the band at 1325 cm^{-1} assigned to the bending of -OH groups in the cellulose component; (vii) the bands at 1163 cm^{-1}, 1112 cm^{-1} 1062 cm^{-1} and 1026 cm^{-1}attributed to the stretching vibration of C-O bonds in alcohols functions [Socrates, 2001]; (viii) a small band at 896 cm^{-1}, due to the C-1 group frequency or ring frequency, characteristic of β-glycosidic bonds between glucose units [Maafi, 2010] and (ix) bands at 705 cm^{-1}, 665 cm^{-1}, 615 cm^{-1} and 561 cm^{-1} assigned to the O-H out of plane deformation vibrations [Socrates, 2001]. The presence of wool and thermo-binder fibres gives rise either to additional vibrations bands on the reinforcement spectrum or to an enhancement of some vibrations. The band at 1718 cm^{-1} attributed to C=O stretching originating from the thermo-binder fibres. Bands at 1314 cm^{-1}, 1571 cm^{-1} are due to carboxylate. There is also a small band observed at 1506 cm^{-1} due to amide II. Furthermore, band at 1242 cm^{-1} is an amide III band. The additional band at 726 cm^{-1} assigned to methylene rocking $-(CH_2)_n-$ originates from PE/PET fibres. The OH and NH stretching in the reinforcement that appeared at 3366 cm^{-1}, is found to be different to OH stretching of the Alfa fibres (3378 cm^{-1}) and the NH stretching of the wool fibres (3310 cm^{-1}). This suggests that hydrogen bonding could have occurred between Alfa, wool and PE/PET fibres. The enhancement of the vibration band intensity at 1648 cm^{-1} is attributed to the contribution of the stretching amide originating from wool fibres. Hence hydrogen bonds occurring between water molecules and wool fibres may decrease the hydrophilic character of the Alfa fibres [Omri, 2013]. Meanwhile, the increase of the band intensity at 1376 cm^{-1} can be explained by a distortion in the glycosidic bond in the cellulose backbone caused by the presence of wool and PE/PET fibres. So, these latter can be considered as surface modifier of Alfa fibres. Indeed, there is also an enhancement of the intensity vibration at 896 cm^{-1} which confirms their effects on Alfa fibres surfaces. Nevertheless, the enhancement of the peaks intensity at 705 cm^{-1}, 665 cm^{-1}, 615 cm^{-1} and 561 cm^{-1} may enhance the hydrophilic character of the reinforcement.

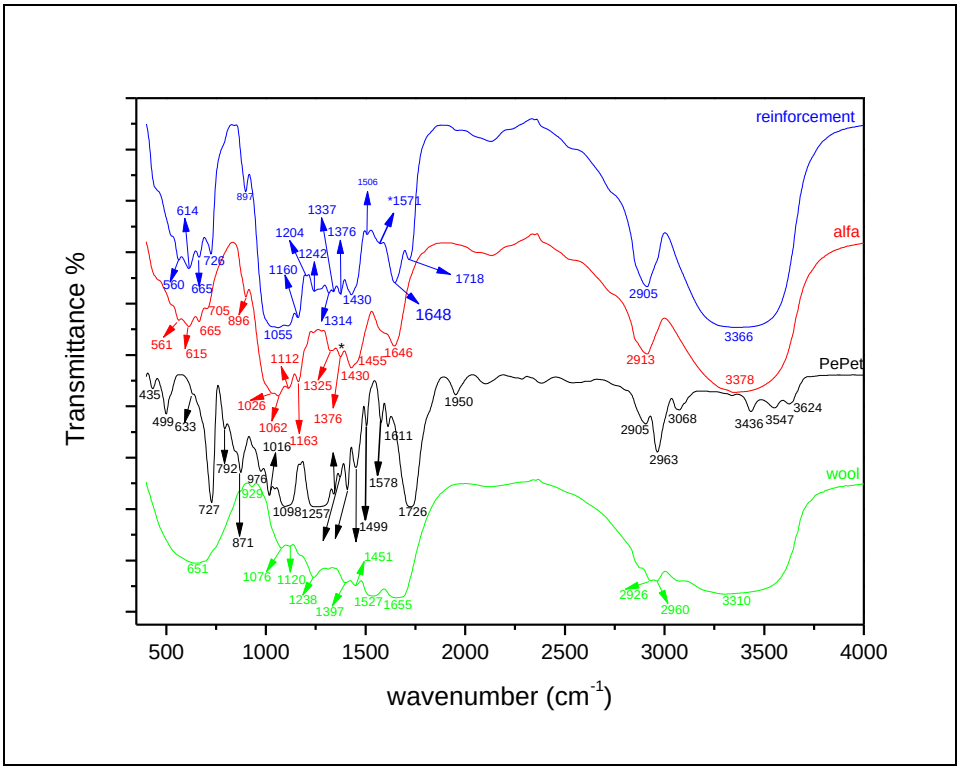

Figure 6: FTIR spectra of Alfa, wool, thermo-binder fibres and the reinforcement in the wavenumber range 400 – 4000 cm^{-1}

So as to analyze the adhesion of Alfa fibres in the matrix, typical FT-IR spectra of the unsaturated polyester matrix and its composite are presented in figure 7. The spectrum of the reinforcement is presented for comparison. The principal absorption peaks obtained for the matrix are as follows: (i) the peaks around

3538 cm^{-1} and 3456 cm^{-1} which can be attributed to the stretching vibrations of hydroxyl (OH) groups; (ii) strong peaks at 3083 cm^{-1}, 3062 cm^{-1}, 3030 cm^{-1} and 2936 cm^{-1}, assigned to C-H stretching; (iii) a very intense peak observed at 1730 cm^{-1} due to the carbonyl (C=O) stretching from the ester linkage; (v) peaks at 1602 cm^{-1}, 1495 cm^{-1}, and 1452 cm^{-1} attributed to the C=C stretching vibrations within the aromatic ring; (vi) band at 1382 cm^{-1} assigned to the symmetric stretching vibrations of the methyl group (-CH_3); (vii) several and strong peaks at 1276 cm^{-1}, 1121 cm^{-1}, 1066 cm^{-1}, and 986 cm^{-1} due to the aromatic C-H in-plane bend and (vii) peaks at 843 cm^{-1}, 746 cm^{-1} and 699 cm^{-1} assigned to the aromatic C-H out-of-plane bend [Coates, 2000].

It is observed that the bands characteristic of the valence vibration of the O–H bond in the matrix at 3456 cm^{-1} and 3538 cm^{-1} are shifted to lower wavelengths, around 3444 cm^{-1} and 3518 cm^{-1} for the composite. As can also be seen in figure 7, this band in the composite is much broader than that of the matrix. This suggests that hydrogen bonding could happen between the matrix and the reinforcement [Silva, Silva, 2005, as shown in the literature Monteiro, Fonseca, 1999]. There is also an intensification of the valence vibration band of the C=O. Indeed the relative intensity of this peak (1730 cm^{-1}) $\left(\frac{I_{composite}}{I_{matrix}}\right)_{C=O}$ is enhanced to 1.25. Figure 8-(a, b) represent the obtained fit of this vibration according to the matrix and the composite, respectively.

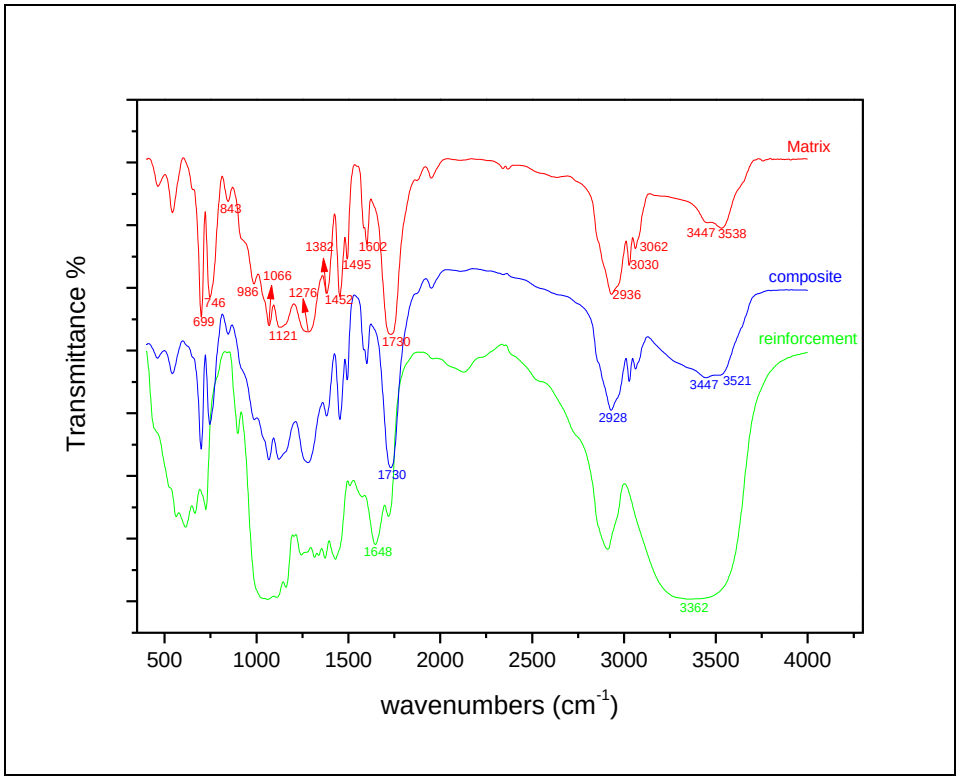

Figure 7: FTIR spectra of the matrix, the reinforcement and the composite in the wavenumber range of 400-4000 cm^{-1}

This indicates that covalent bonding has taken place through an esterification reaction between the fibers OH groups and unsaturated polyester COOH groups [Moyeenuddin, 2011]. Hence, the absence of the vibration at 1648 cm^{-1} allows such interaction between the reinforcement and the matrix. Nevertheless, the presence of the water dipoles polarization as mentioned in the DEA section revealed the presence of moisture structure in the reinforcement. Indeed, it is known that the lignocellulosic absorbs water by forming hydrogen bonding between water and hydroxyl groups of cellulose, hemicellulose and lignin in the cell wall [Roman, 2000].

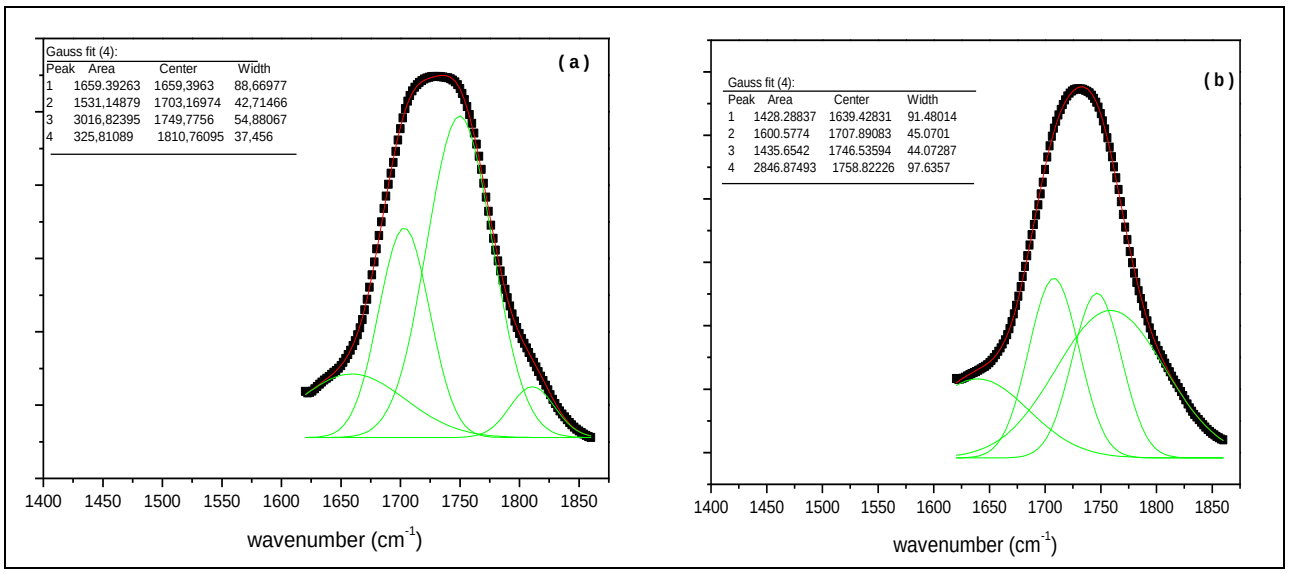

Figure 8: Peak Fit of carbonyl stretch situated in 1730 cm^{-1} in matrix (a) and composite (b)

3.3. SEM

SEM micrographs of the polished cross-sections for the composite are displayed in figure 9-(a, b, c, c, d). Figure 9-(a, b) shows the fibre distribution in the composite. We can observe different shaped cross-sections. Indeed, fibres tend to agglomerate in the composite. This may be due to hydrogen bonding between fibres surface, brought by the hydroxyl groups as evidenced by the FTIR analysis.

Such heterogeneity confirms the statistical analysis of the interfacial polarization effect, which is consistent with the Havriliak-Negami process. Nevertheless, these irregularities may produce deleterious effect on the interfacial region fibres/matrix. In fact, figure 9-(c, d) shows different close contact in the interfacial region between the fibre and the matrix. We can also notice the evidence of crack path propagates through the interfacial region. This may result from non-homogeneous distribution of wool and PE/PET fibres at the interfacial region.

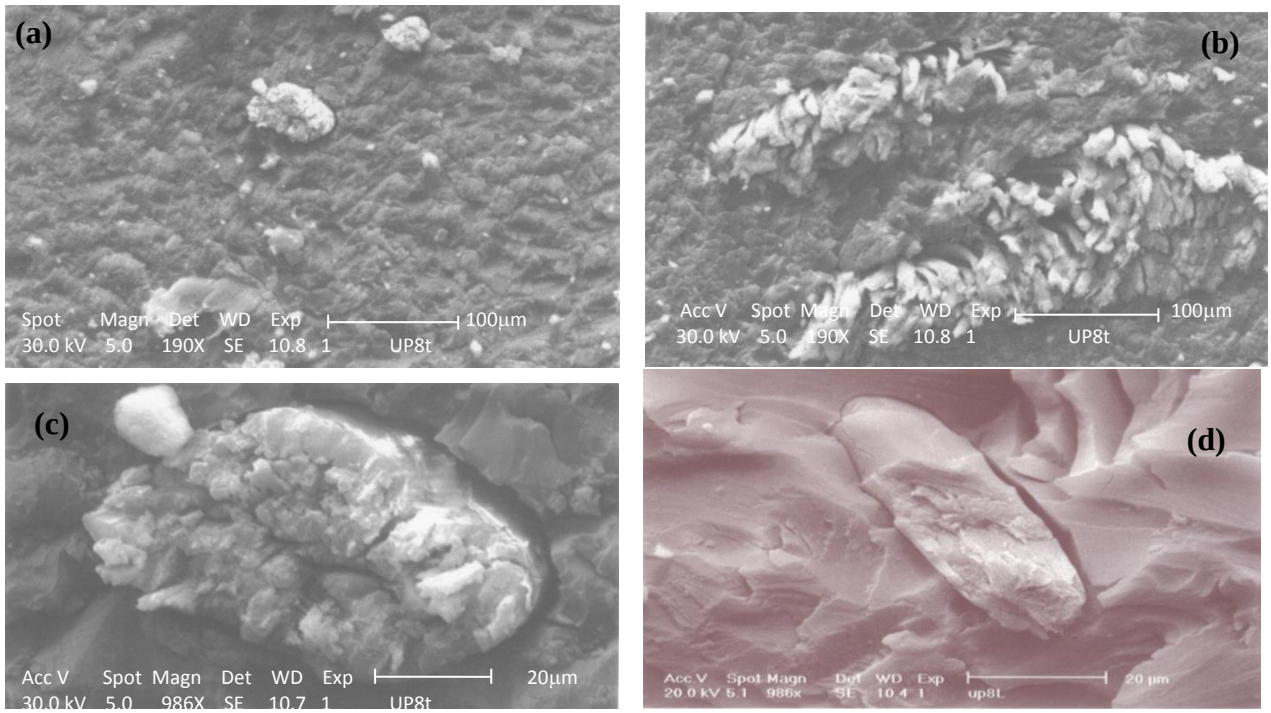

Figure 9. SEM micrographs of the polished cross-sections for the composite: 100 µm (a, b) and 20 µm (c, d).

4. CONCLUSION

Dielectric measurements were performed on Alfa fibres reinforced unsaturated polyester composite taking into account the presence of wool and thermo-binder fibres. This dielectric study revealed the presence of water dipoles polarization at low temperatures and the interfacial polarization effect at high temperatures. Due to the enhancement of ionic conduction at high temperatures, MWS polarization effect was analysed using the electric modulus formalism and according to the Havriliak-Negami model. This polarization effect revealed a low strength attributed to a chemical interaction between the reinforcement and the matrix. Vibrational study revealed that wool and thermo-binder fibres provided an adhesion mechanism based on covalent bonds and hydrogen bridges despite of the moisture structure of the reinforcement. SEM observation confirmed that close contact could occur between fibres and the matrix. Nevertheless, heterogeneous fibre distribution might influence the interfacial region.

REFERENCES

Arous, M., Ben Amor, I., Boufi, S., Kallel, A. (2007). Experimental Study on Dielectric Relaxation in Alfa Fiber Reinforced Epoxy Composites.J. Appl. Polym. Sci., 106, 3631-3640.

Aziz, SH., Ansell, MP., Clarke, SJ., Panteny, SR. (2005). Modified polyester resins for natural fibre composites, Compos Sci Technol 65:525–535

Belaabed, B., Wojkiewicz, JL., Lamouri, S., El Kamchi, N., Redon, N. (2011). Thermomechanical behaviors and dielectric properties of polyaniline-doped para-toluene sulfonic acid/epoxy resin composites. Polym. Adv. Technol., 23:1194-2200.

Bisanda, ETN., Anshell, MP. (1991). The effect of silane treatment on the mechanical and physical properties of sisal-epoxy composites. Compos Sci Technol 41:165-178.

Coates, J. (2000). Interpretation of Infrared Spectra, A Practical Approach, edited by R. A. Meyers (John Wiley & Sons Ltd, Chichester), p. 10815

Colom, X., Carrasco, F., Pagès, P., Canavate, J. (2003). Effects of different treatments on the interface of HDPE/lignocellulosic fiber composites. Compos. Sci. and Technol. 63, 161-169.

Ermolaeva, NS., Kaveline, KG., Spoormaker, JL. (2002). Materials selection combined with optimal structural design: concept and some results. Mater Des 23:459–70.

Ghallabi, Z., Rekik, H., Boufi, S., Arous, M., Kallel, A. (2010). Effect of the interface treatment on the dielectric behaviour of composite materials of unsaturated polyester reinforced by alfa fiber. J. Non-Crystalline Solids 356:684-687.

Guicha, M. (2009). Optimisation des structures textiles à base de fibres d'alfa, *Master Thesis, Université de Monastir, Ecole Nationale d'ingénieurs de Monastir.*

Havriliak, S., Negami, S. (1966). A complex plane analysis of Alpha-dispersion in some polymer systems. J. Polym. Sci., Part C: J. Polym. Symp. 14 99–117.

Howard, W., Starkweather, JR., Avakian, P. (1992) Conductivity and the electric modulus in polymers, Journal of Polymer Science:Part B30:637-641 (1992).

Laly, AP., Sabu, T. (2003). Polarity parameters and dynamic mechanical behaviour of chemically modified banana fibre reinforced polyester composites. Comp Sci Technol 63:1231-1240.

Maafi, EM., Malek, F., Tighzert, L., Dony, P. (2010). Synthesis of Polyurethane and Characterization of its Composites Based on Alfa Cellulose Fibers. J Polym Environ DOI 10.1007/s10924-010-0218-8.

Mishra, S., Mohanty, AK., Drzal, LT., Misra, M., Parija, S., Nayak, SK., Tripathy, SS. (2003). Studies on mechanical performance of biofibre/glass reinforced polyester hybrid composites, Compos. Sci. and Technol, 63, 1377–1385.

Monteiro, EEC., Fonseca, JLC. (1999), Stress relaxation of thermoplastic polyurethanes monitored by FTIR spectroscopy, Polym Test 18:281-286.

Puertolas, JA., Castro, M., Telleria, I., Algeria, A. (1999). Analysis of the relaxation on polymers from the real part of a general complex susceptibility : Application to dielectric relaxation. J. Polym. Sci. : Part B37:1337-1349.

Roman, HD., Tan, KW., Kumar, RN., Abubakar, A., Ishak, ZAM., Ismail, H. **(2000)**. The effect of lignin as a compatibilizer on the physical properties of coconut fiber-polypropylene composites, European Polym. J. 36:1483-1494.

Silva, MC., Silva, GG. (2005). A new composite from cellulose industrial waste and elastomeric polyurethane, J Appl Polym Sci 98:336-340.

Socrates, G. (2001). Infrared and Raman Characteristic Group Frequencies/Tables and Charts, 3rd ed.; John Wiley & Sons Ltd : Baffins Lane, Chichester, West Sussex PO19 IUD, England, pp .1-343.

Sun, XF., Xu, F., Sun, RC., Fowler, P., Baird, MS. (2005). Characteristics of degraded cellulose obtained from steam-exploded wheat straw. Carbohyd. Res. 340, 97–106.

Triki, A., Guicha, M., Ben Hassen, M., Arous, M., Fakhfakh, Z. (2011). Studies of Dielectric Relaxation in Natural Fibres Reinforced Unsaturated Polyester. J. Mater. Sci., 46,3698–3707.

TRIKI, A., OMRI, MA., GUICHA, M., BEN HASSEN, M., AROUS, M., KALLEL, A. (2013). Correlation between mechanical and dielectric properties of Alfa/Wool/Polymeric hybrid fibres reinforced polyester composites, 7th EEIGM International Conference on Advanced Materials Research, IOP Conf. Series: Materials Science and Engineering 48, 012008 doi:10.1088/1757-899X/48/1/012008

Omri, MA., Triki, A., Guicha, M., Ben Hassen, M., Arous, M., El Hamzaoui, HA., Bulou, A. **(2013).** Effect of wool and thermo-binder fibers on adhesion of alfa fibers in polyester composite. J. Appl. Physics. 114, 224105.

Wagner, H., Richert, R. (1999). Measurement and analysis of time-domain electric field relaxation : the vitreous ionic conductor 0.4Ca(NO3)2-0.6KNO3. J. Appl. Phys. 85, 1750–1755.